

Supplementary Information for

Bismuth Oxide: A Versatile High-Capacity Electrode Material for Rechargeable Aqueous Metal-Ion Batteries†

Wenhua Zuo,^{a,b} Weihua Zhu,^a Dengfeng Zhao,^b Yunfei Sun,^c Yuanyuan Li,^c Jinping Liu^{*,a,b}
and Xiong Wen (David) Lou^{*,d}

^a School of Chemistry, Chemical Engineering and Life Science and State Key Laboratory of Advanced Technology for Materials Synthesis and Processing, Wuhan University of Technology, Wuhan, Hubei 430070, P. R. China. Email: liujp@whut.edu.cn

^b Institute of Nanoscience and Nanotechnology, Department of Physics, Central China Normal University, Wuhan, Hubei 430079, P. R. China

^c School of Optical and Electronic Information, Huazhong University of Science and Technology, Wuhan 430074, P. R. China

^d School of Chemical and Biomedical Engineering, Nanyang Technological University, 62 Nanyang Drive, Singapore, 637459, Singapore. Email: davidlou88@gmail.com

† Electronic supplementary information (ESI) available. See DOI: XXX/XXXX

Calculation methods of discharge capacity and ion diffusion coefficient.

The specific discharge capacity from CV measurement was calculated according to the equation:

$$Q = \frac{\int I(V) \times dV}{\nu m}$$

Where $I(V)$ is the current at V , dV is the differential potential, ν is the scan rate and m is the mass of active material. And the specific discharge capacity from galvanostatic method was calculated according to the equation:

$$Q = \frac{I \times \Delta t}{m}$$

Where I and Δt represent the discharging current and time, respectively. All ion diffusion coefficients were calculated based on the following equation:

$$D = \frac{R^2 T^2}{2 A^2 n^4 F^4 C^2 \sigma^2}$$

Where R is the gas constant ($8.314472 \text{ J}\cdot\text{K}^{-1}\cdot\text{mol}^{-1}$), T is the room temperature (298.15 K); A is the surface area of the electrode (2 cm^2); n is the number of electrons transferred (1); F is the Faraday constant ($96485.33 \text{ C mol}^{-1}$) and C is the concentration of generated OH^- ions. While σ represents the slope of the plot of Z_{Re} against $\omega^{1/2}$ based on the equation:

$$Z_{Re} = R_s + R_{ct} + \sigma \omega^{-1/2}.$$

Figures:

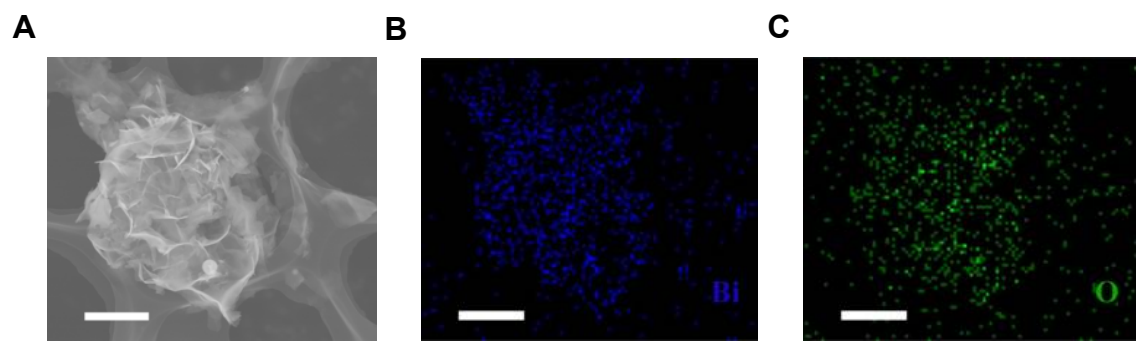


Fig. S1. EDS elemental mapping analysis. (A) SEM image of Bi_2O_3 nanoflake clusters scraped from Ti substrate. (B, C) The corresponding elemental distribution of Bi and O, respectively. Scale bar, 1 μm .

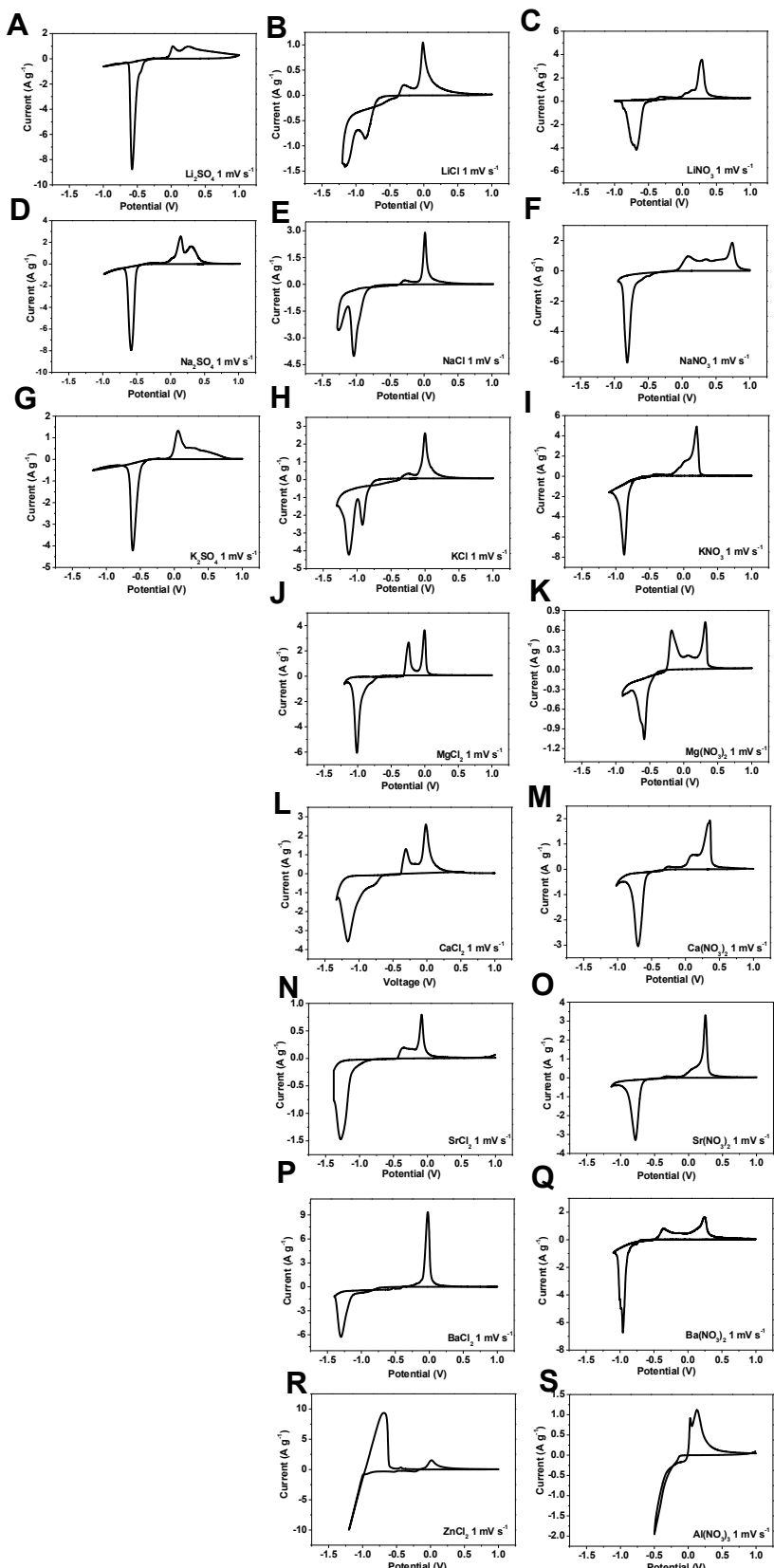


Fig. S2. CV curves at 1 mV s^{-1} in different electrolytes. All potential in this figure is vs. SCE.

(A) 0.5 M Li_2SO_4 . (B) 1 M LiCl . (C) 1 M LiNO_3 . (D) 0.5 M Na_2SO_4 . (E) 1 M NaCl . (F) 1 M NaNO_3 . (G) 0.5 M K_2SO_4 . (H) 1 M KCl . (I) 1 M KNO_3 . (J) 1 M MgCl_2 . (K) 1 M $\text{Mg}(\text{NO}_3)_2$. (L) 1 M CaCl_2 . (M) 1 M $\text{Ca}(\text{NO}_3)_2$. (N) 1 M SrCl_2 . (O) 1 M $\text{Sr}(\text{NO}_3)_2$. (P) 1 M BaCl_2 . (Q) 1 M $\text{Ba}(\text{NO}_3)_2$. (R) 1 M ZnCl_2 . (S) 1 M $\text{Al}(\text{NO}_3)_3$.

(L) 1 M CaCl_2 . (M) 1 M $\text{Ca}(\text{NO}_3)_2$. (N) 1 M SrCl_2 . (O) 1 M $\text{Sr}(\text{NO}_3)_2$. (P) 1 M BaCl_2 . (Q) saturated $\text{Ba}(\text{NO}_3)_2$. (R) 1 M ZnCl_2 with 5.833 $\text{mL}\cdot\text{L}^{-1}$ hydrochloric acid. (S) 1 M $\text{Al}(\text{NO}_3)_3$.

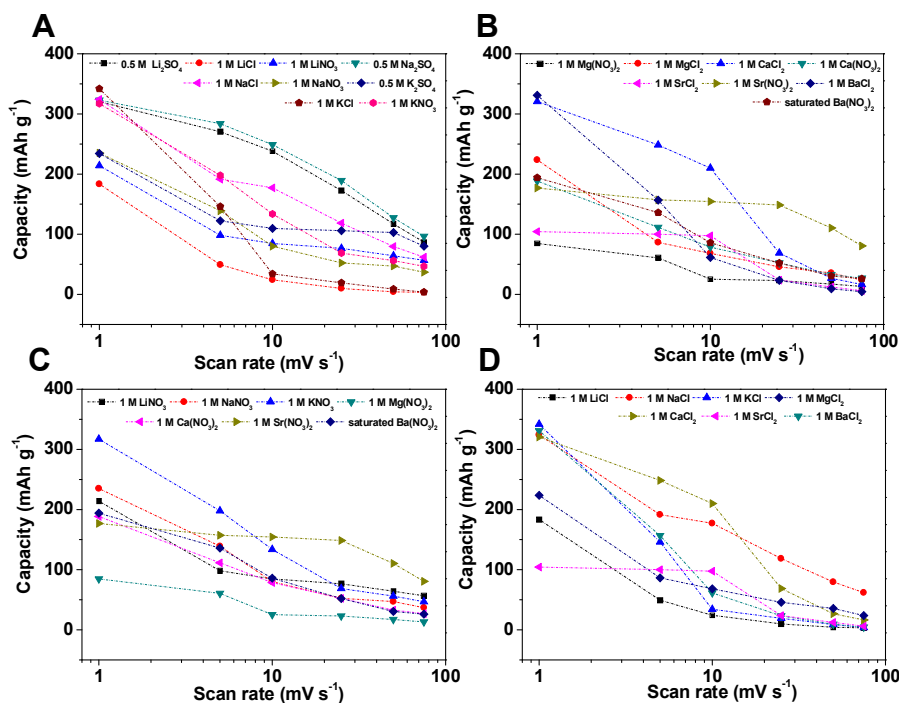


Fig. S3. Separate CV rate performance comparison for Bi_2O_3 electrode. CV rate performance comparison in (A) monovalent metal nitrate/chloride/sulfate electrolytes; (B) divalent metal nitrate/chloride electrolytes; (C) mono-/divalent metal nitrate electrolytes; (D) mono-/divalent metal chloride electrolytes.

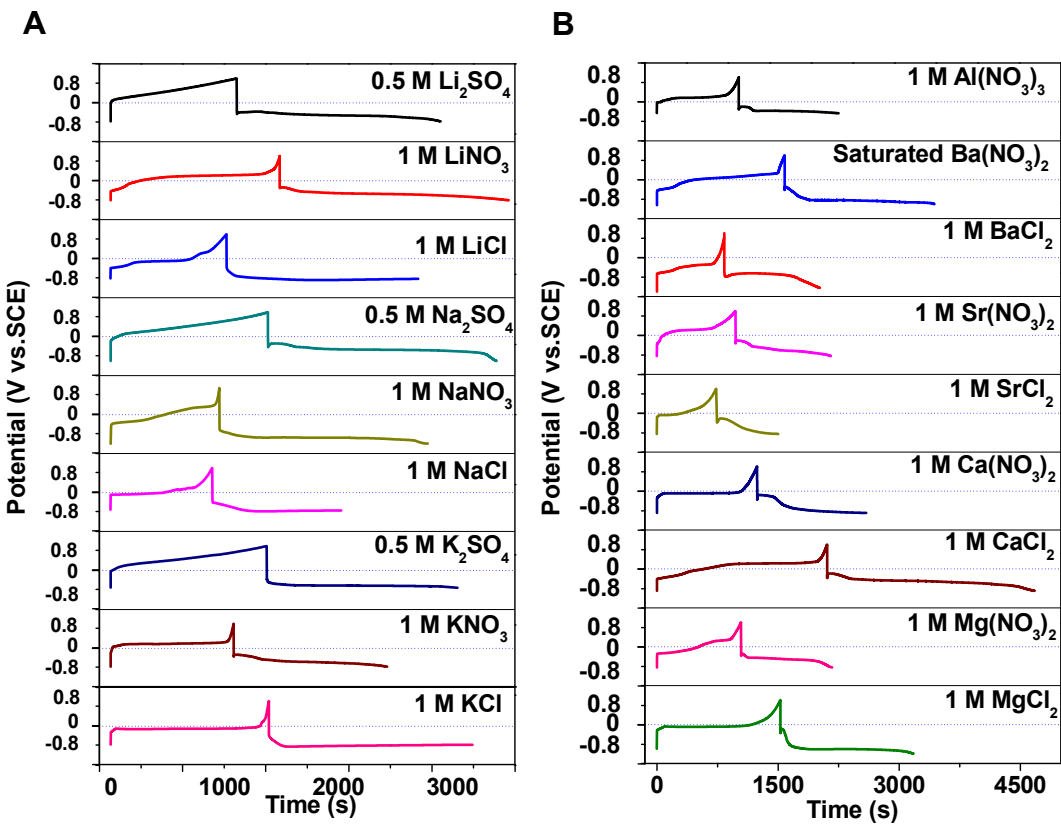


Fig. S4. Galvanostatic charge-discharge performance of Bi_2O_3 electrode at 0.5 A g^{-1} . All potential in this figure is vs. SCE. (A) in monovalent cation aqueous electrolytes. (B) in multivalent cation electrolytes.

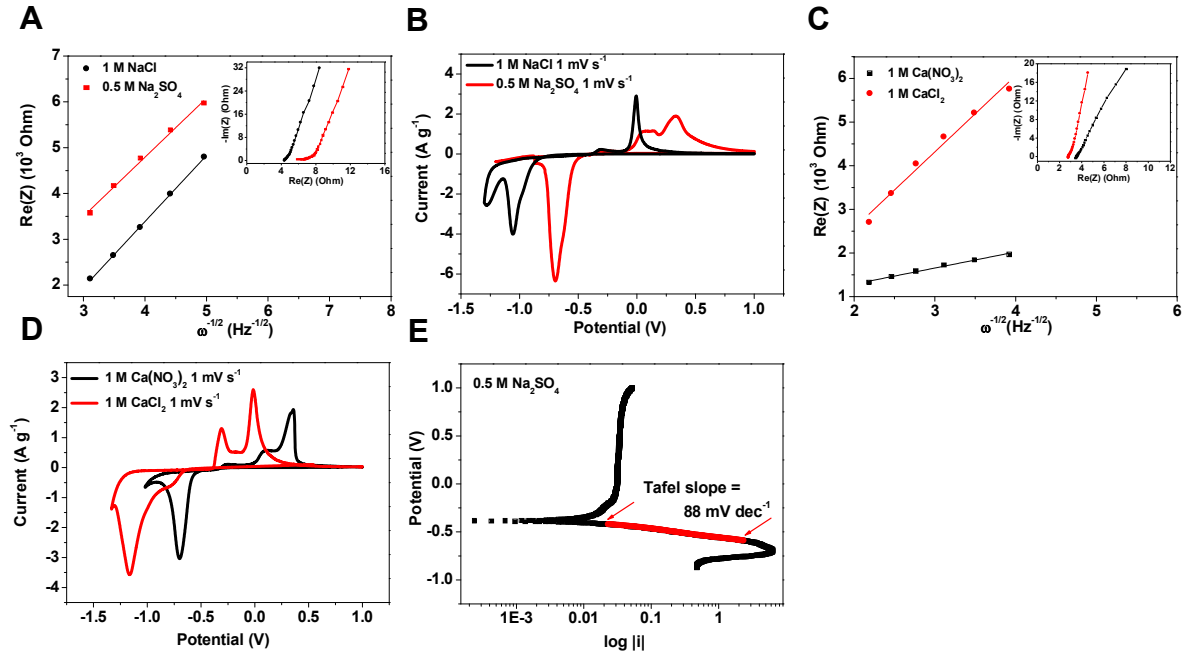


Fig. S5. Electrolyte influence on the electrochemical kinetics. (A) Plots of Z_{Re} against $\omega^{1/2}$ in $0.5 \text{ M Na}_2\text{SO}_4$ and 1 M NaCl . The inset shows the corresponding Nyquist plots. (B) CV curve comparison of Bi_2O_3 electrode at 1 mV s^{-1} in $0.5 \text{ M Na}_2\text{SO}_4$ electrolyte and 1 M NaCl electrolyte. (C) Plots of Z_{Re} against $\omega^{1/2}$ in $1 \text{ M Ca}(\text{NO}_3)_2$ and 1 M CaCl_2 , The inset shows the corresponding Nyquist plots. (D) CV curve comparison of Bi_2O_3 electrode at 1 mV s^{-1} in $1 \text{ M Ca}(\text{NO}_3)_2$ electrolyte and 1 M CaCl_2 electrolyte. (E) Tafel plot in $0.5 \text{ M Na}_2\text{SO}_4$ electrolyte, showing the cathodic Tafel slope of 88 mV dec^{-1} .

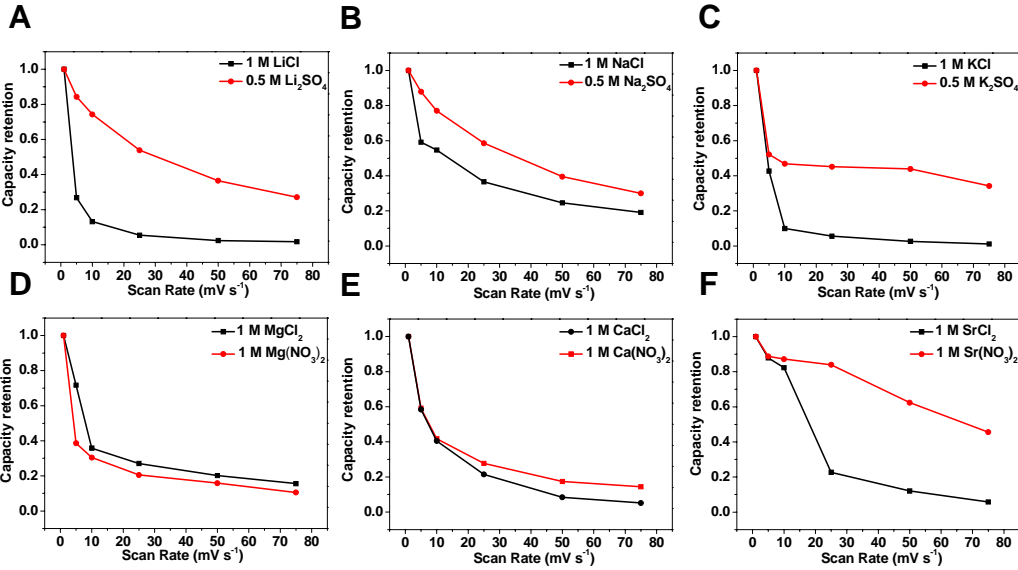


Fig. S6. Rate performance comparison for Bi_2O_3 electrode in electrolytes with the same cation but different anions.

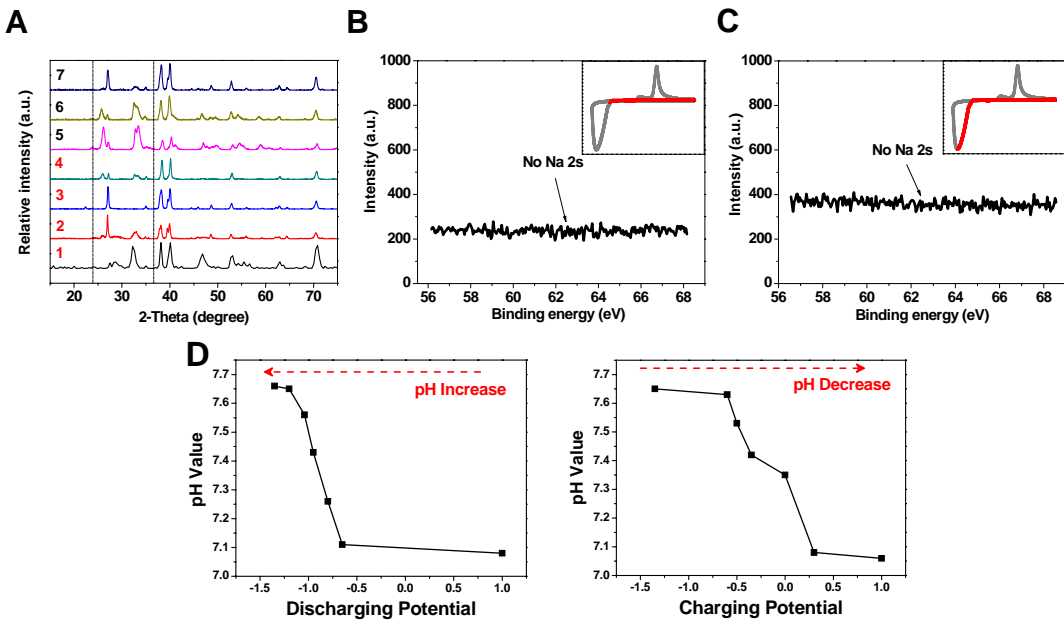


Fig. S7. Additional data for energy storage mechanism analysis. (A) Ex-situ full XRD patterns of the electrode at various electrochemical stages of 1-7. (B-C) Na 2s XPS spectrum of the electrode cathodically swept over -0.93 and -1.24 V in mixed Na^+ electrolyte at 10 mV s⁻¹, respectively. The results clearly demonstrate the absence of Na^+ . (D) pH value change trend around the Bi_2O_3 electrode during charging and discharging. It is found that during discharging the pH value increases while during charging it decreases, further supporting our proposed electrochemical mechanism.

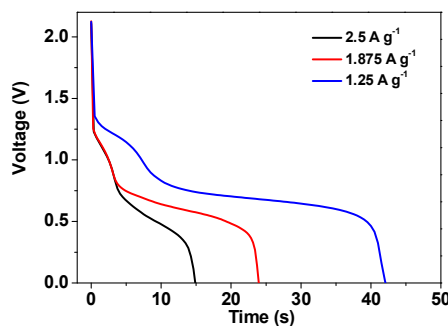


Fig. S8. The discharge curves of LiMn₂O₄//(slurry)Bi₂O₃ full cell. At current densities of 1.25, 1.875 and 2.5 A g⁻¹.

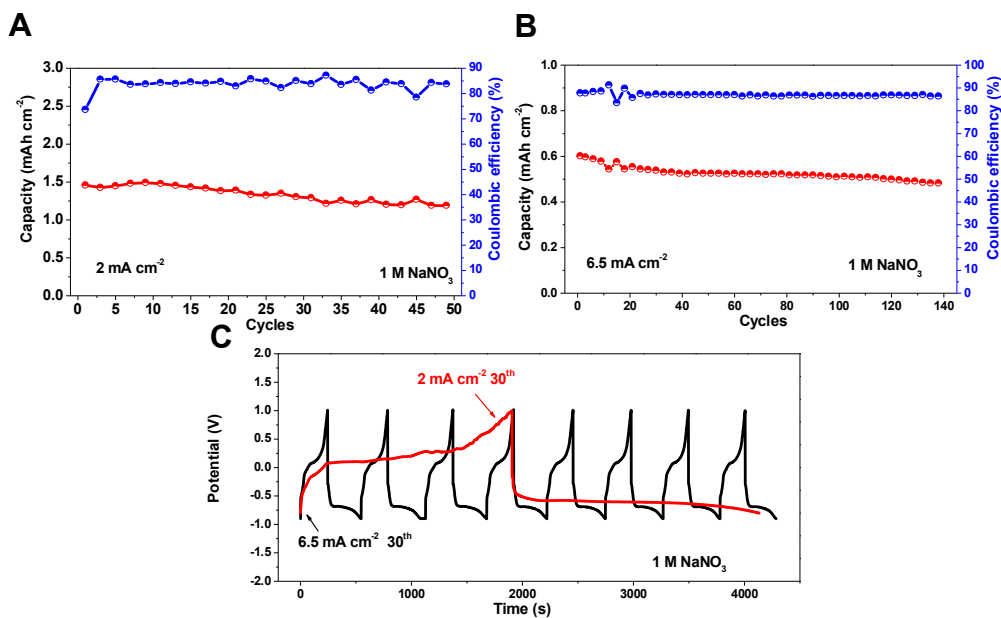


Fig. S9. Cycling stability of high areal mass loading electrode in NaNO₃ electrolyte. (A) at 2 mA cm⁻²; (B) at 6.5 mA cm⁻². (C) Comparison of the charge-discharge curves. The electrode was firstly activated at 10 mV s⁻¹ for 10 cycles.

Table S1. Electrode discharge capacities and pH values in various electrolytes. CV testing was applied at 1mV s^{-1} and galvanostatic charge-discharge (CD) testing at 0.5 A g^{-1} .

Electrolytes		pH values	CV capacity (mAh g ⁻¹)	CD capacity (mAh g ⁻¹)
Li ⁺	SO ₄ ²⁻	7.08	320	248
	Cl ⁻	7.03	183	234
	NO ₃ ⁻	7.41	214	278
Na ⁺	SO ₄ ²⁻	7.16	322	278
	Cl ⁻	7.06	324	157
	NO ₃ ⁻	7.26	235	255
K ⁺	SO ₄ ²⁻	6.90	234	232
	Cl ⁻	6.91	342	248
	NO ₃ ⁻	7.10	317	186
Mg ²⁺	Cl ⁻	7.03	223	228
	NO ₃ ⁻	6.62	84	156
Ca ²⁺	Cl ⁻	7.52	321	356
	NO ₃ ⁻	7.23	188	187
Sr ²⁺	Cl ⁻	7.00	104	106
	NO ₃ ⁻	7.41	177	164
Ba ²⁺	Cl ⁻	7.27	331	165
	NO ₃ ⁻	7.46	194	258
Al ³⁺	NO ₃ ⁻	2.58	-	171

Table S2. Effective radii of ions.

Ions	Crystal Radii (Å)	Hydrated Radii (Å)
Li ⁺	0.60	3.82
Na ⁺	0.95	3.58
K ⁺	1.33	3.31
Mg ²⁺	0.65	4.28
Ca ²⁺	0.99	4.12
Sr ²⁺	1.13	4.12
Ba ²⁺	1.35	4.04
Cl ⁻	1.81	3.32
NO ₃ ⁻	2.64	3.35
SO ₄ ²⁻	2.90	3.79

Table S3. EIS analysis of the Bi₂O₃ electrode in various electrolytes.

Electrolytes		R_s (Ω)	σ	D_{OH^-} (10^{-7} cm ² s ⁻¹)	Tafel slope (mV dec ⁻¹)
Li ⁺	SO ₄ ²⁻	6.67	767	4.72	101
	Cl ⁻	4.52	2018	0.54	243
Na ⁺	SO ₄ ²⁻	5.62	1251	2.57	88
	Cl ⁻	4.36	1498	1.13	254
K ⁺	SO ₄ ²⁻	4.56	623	3.13	55
	Cl ⁻	4.05	3982	0.08	76
Mg ²⁺	Cl ⁻	2.68	1680	0.78	91
	NO ₃ ⁻	3.38	2455	0.06	143
Ca ²⁺	Cl ⁻	2.80	1749	6.89	204
	NO ₃ ⁻	3.52	368	40.9	152
Sr ²⁺	Cl ⁻	2.73	2550	0.30	309
	NO ₃ ⁻	3.68	604	37.8	91

Note S1. The calculation of theoretical specific capacity.

$$Q = \frac{nF}{m}$$

n: the number of electrons transferred, in this study is 6;

F: Faraday constant 96485.33 C mol⁻¹;

m: the relative molecular mass 465.96 g mol⁻¹.

Thus, $Q = 345.11$ mAh g⁻¹.